Electronic Supplementary Material (ESI) for Chemical Science.

Supporting information

Residue-specific identification of phase separation hot spots of Alzheimer-related protein Tau

Susmitha Ambadipudi,[a] Jithender G. Reddy,[b,c] Jacek Biernat,[d] Eckhard Mandelkow,[d,e] and Markus Zweckstetter*[a,b]

a. Deutsches Zentrum für Neurodegenerative Erkrankungen (DZNE), Von-Siebold-Str. 3a, 37075 Göttingen, Germany
b. Max-Planck-Institut für Biophysikalische Chemie, Am Fassberg 11, 37077 Göttingen, Germany.
c. NMR & Structural Chemistry Division, CSIR-Indian Institute of Chemical Technology, Hyderabad, 500007, India.
d. Deutsches Zentrum für Neurodegenerative Erkrankungen (DZNE), Ludwig-Erhard-Allee 2, 53175 Bonn, Germany.
e. CAESAR Research Center, Bonn, and MPI for Metabolism Research, Hamburg Outstation, 22607 Hamburg, Germany.

*Correspondence: Address all correspondence and requests for materials to: M.Z (E-mail: mazw@nmr.mpibpc.mpg.de)

Table of Contents Page No

Figure S1. Superposition of temperature-dependent $^{1}H/^{15}N$ HSQC spectra 3

Figure S2. Quantitative estimation of K18 in the droplet and dispersed phase 4

Figure S3. Effect of the addition of 1,6-hexanediol on the chemical shifts of dispersed K18 at 5 °C 5

Figure S4. Spectral comparison of KXGS motifs 6

Figure S5. Superposition of 2D CBCACO spectra in dispersed and LLPS state 7

Figure S6. Secondary chemical shifts of CO in droplet and dispersed phase 8

Table S1. Acquisition parameters of triple-resonance NMR experiments 9

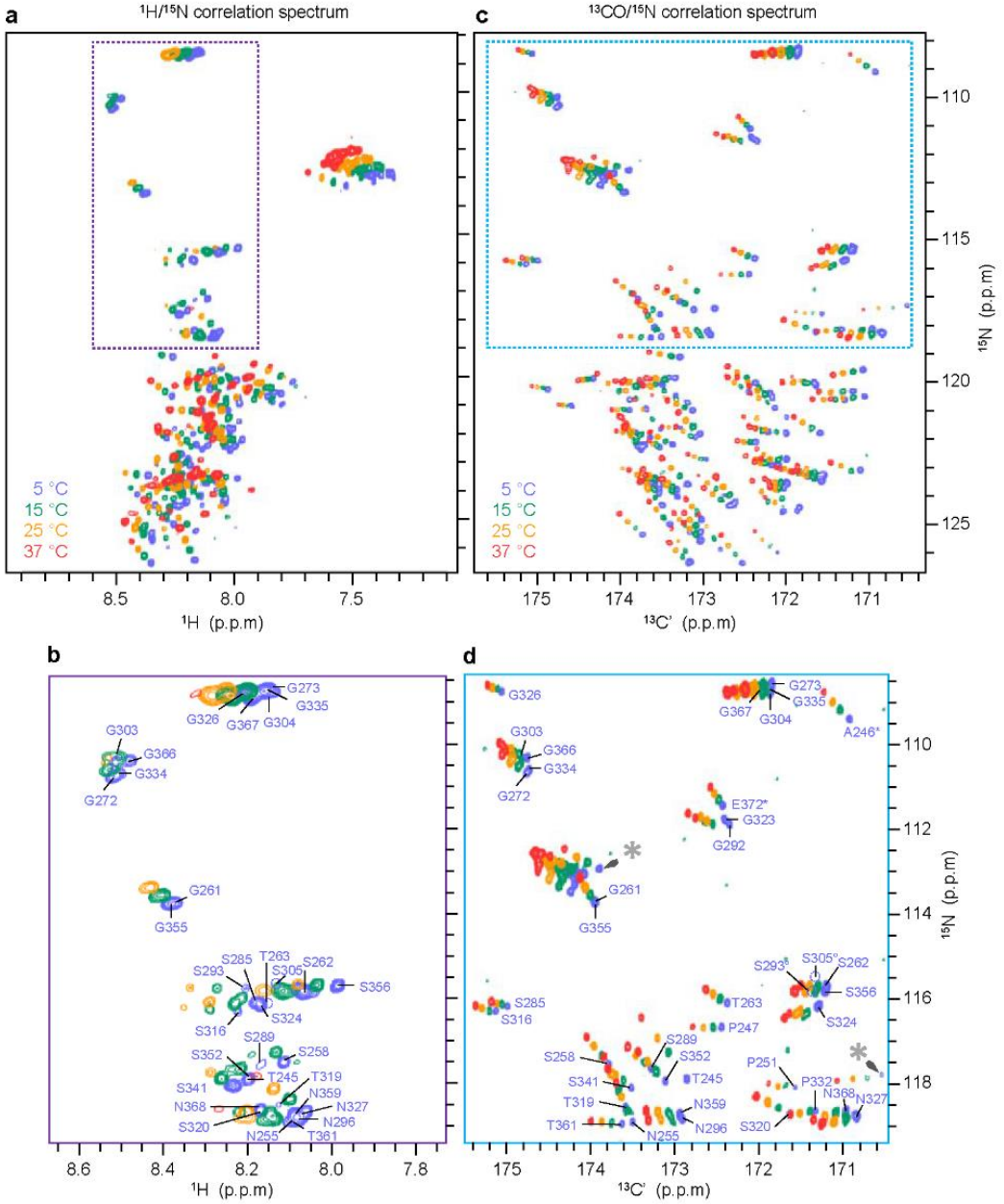

Figure S1. Superposition of temperature-dependent $^{1}H/^{15}N$ HSQC spectra (a,b) and CON spectra (c,d) of K18. (b) and (d) are selected regions boxed in (a) and (b), respectively. Upon liquid-liquid phase separation at 37 °C, many cross-peaks in the $^{1}H/^{15}N$ HSQC spectrum strongly broadened (i.e. no cross peak visible in the red spectrum shown in (a,b) at 37 °C). Cross-peaks marked by a star in the CON spectrum remained unassigned.

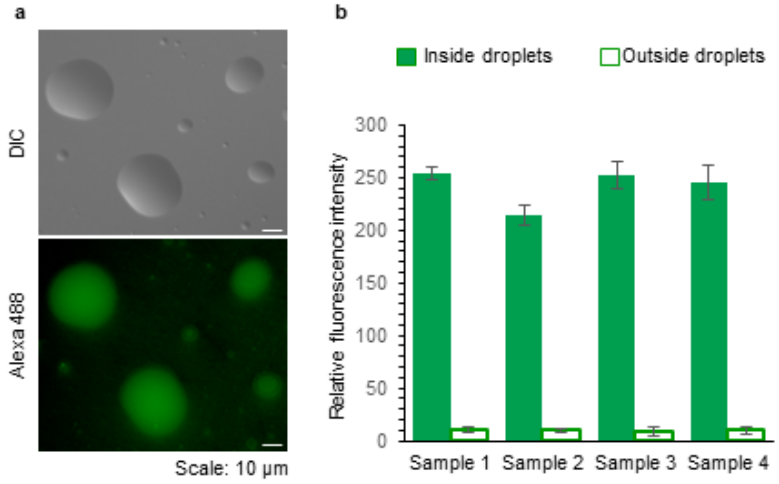

Figure S2. Quantitative estimation of K18 in the droplet and dispersed phase. (a) DIC (top panel) and fluorescence microscopy (bottom panel) of K18 droplets. (b) Relative fluorescence intensities of Alexa 488 labeled K18 in droplets (filled bars) and the surrounding environment (hollow bars) from four independent measurements.

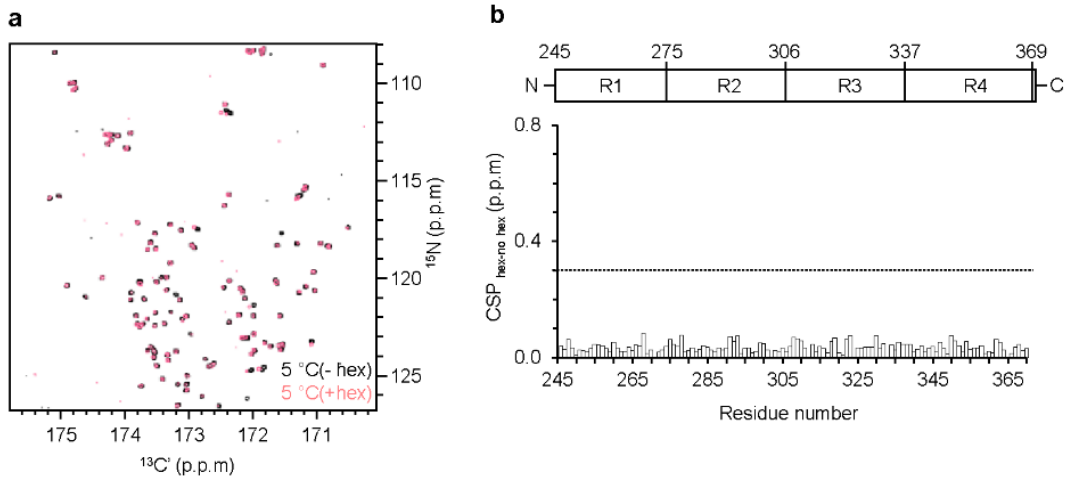

Figure S3. Effect of the addition of 1,6-hexanediol on the chemical shifts of dispersed K18 at 5 °C. (a) Superposition of CON spectra of K18 in the monomeric dispersed state (5 °C) in the absence (black) and presence (pink) of 1,6-hexanediol. (b) Averaged chemical shift perturbation ($CSP_{hex\text{-}no\ hex}$) of CO and N obtained from spectra overlaid in (a).

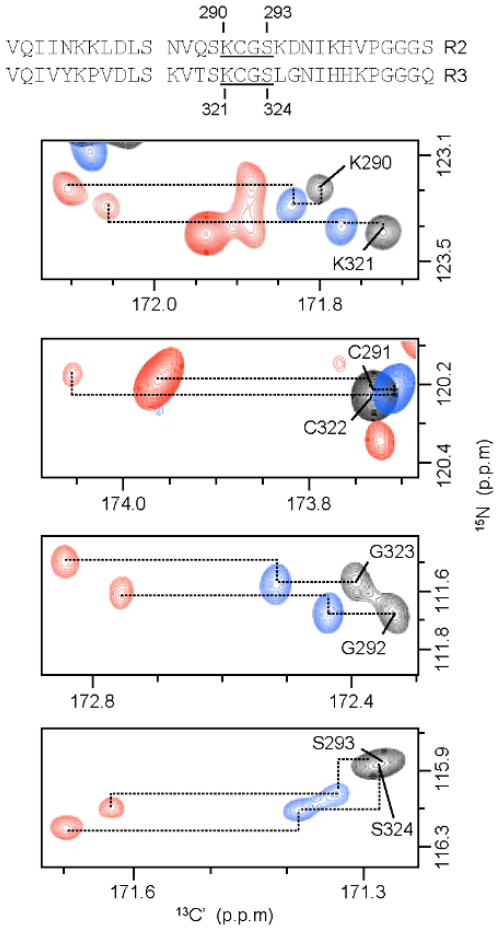

Figure S4. Spectral comparison of KXGS motifs (in repeats R2 and R3) in the monomeric dispersed state (5 °C, black), the LLPS state (37 °C, red) and droplet-dissolved state (37 °C with 1,6-hexanediol, blue).

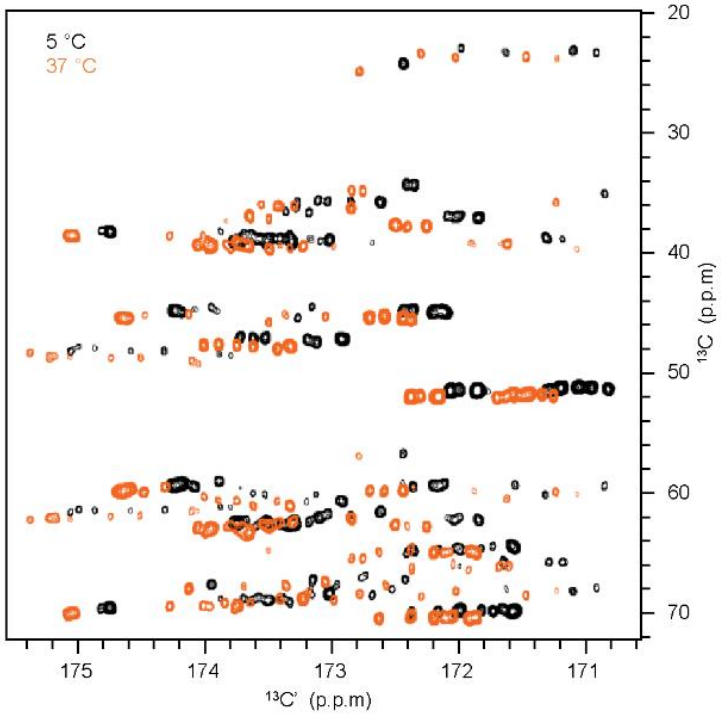

Figure S5. Superposition of 2D CBCACO spectra of K18 in the monomeric dispersed state (5 °C, black) and LLPS state (37 °C, orange).

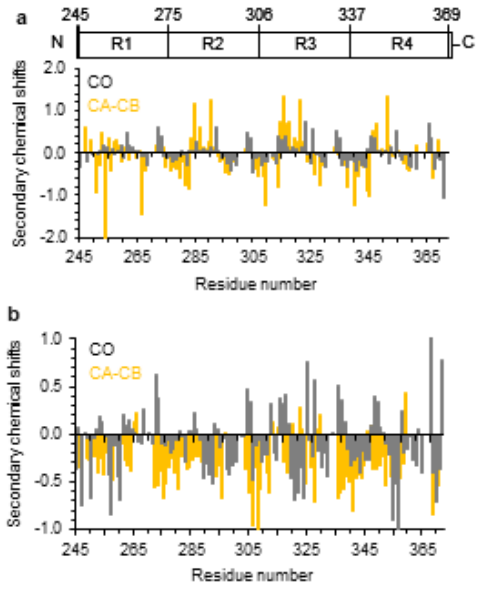

Figure S6. Secondary chemical shifts of K18 at 37 °C in (a) the droplet (- hex, i.e. without 1,6-hexanediol) and (b) the dispersed state (+ hex). Secondary chemical shifts are calculated as difference between observed and random coil chemical shifts. (a) In the absence of 1,6-hexanediol, CO and (CA-CB) (same as in Fig. 2e) show a similar sequence dependence in secondary chemical shifts. (b) More negative values of secondary chemical shifts in the dispersed phase (+ hex) indicates a higher tendency for extended conformation.

Table S1. Acquisition parameters of triple-resonance NMR experiments.

	Dimension (nucleus)			**Spectral width (offset), ppm**			**Scans**
Experiment	***t1***	***t2***	***t3***	**F1**	**F2**	**F3**	***n***
HNCO	80 (13C)	64 (15N)	2048 (1H)	7.0 (172.5)	19.0 (117.5)	12.0 (4.7)	8
HN(C)N	64 (15N)	64 (15N)	2048 (1H)	19.0 (117.5)	19.0 (117.5)	12.0 (4.7)	16
HNCACB	80 (13C)	48 (15N)	2048 (1H)	53.0 (46.0)	19.0 (117.5)	12.0 (4.7)	16
HN(CO)CACB	80 (13C)	48 (15N)	2048 (1H)	53.0 (46.0)	19.0 (117.5)	12.0 (4.7)	8